

Journal Pre-proof

Improved efficacy of FKRP AAV gene therapy by combination with ribitol treatment for LGMD2I

Marcela P. Cataldi, Charles H. Vannoy, Anthony Blaeser, Jason D. Tucker, Victoria Leroy, Raegan Rawls, Jessalyn Killilee, Molly C. Holbrook, Qi Long Lu

PII: S1525-0016(23)00599-3

DOI: <https://doi.org/10.1016/j.ymthe.2023.10.022>

Reference: YMTHE 6222

To appear in: *Molecular Therapy*

Received Date: 11 July 2023

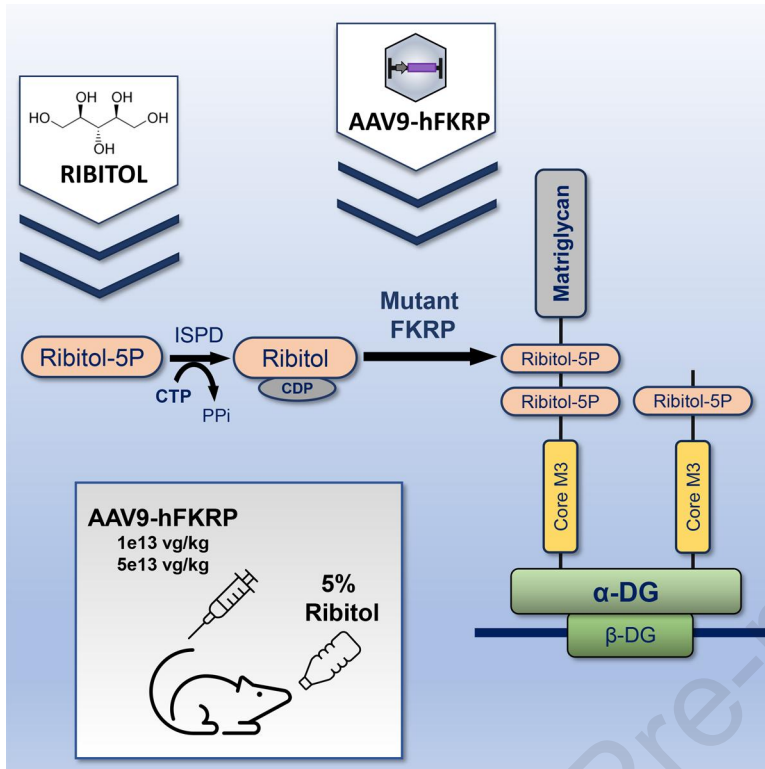
Accepted Date: 31 October 2023

Please cite this article as: Cataldi MP, Vannoy CH, Blaeser A, Tucker JD, Leroy V, Rawls R, Killilee J, Holbrook MC, Lu QL, Improved efficacy of FKRP AAV gene therapy by combination with ribitol treatment for LGMD2I, *Molecular Therapy* (2023), doi: <https://doi.org/10.1016/j.ymthe.2023.10.022>.

This is a PDF file of an article that has undergone enhancements after acceptance, such as the addition of a cover page and metadata, and formatting for readability, but it is not yet the definitive version of record. This version will undergo additional copyediting, typesetting and review before it is published in its final form, but we are providing this version to give early visibility of the article. Please note that, during the production process, errors may be discovered which could affect the content, and all legal disclaimers that apply to the journal pertain.

© 2023 The American Society of Gene and Cell Therapy.





1 **Improved efficacy of FKRP AAV gene therapy**
2 **by combination with ribitol treatment**
3 **for LGMD2I**
4

5 Marcela P. Cataldi¹, Charles H. Vannoy, Anthony Blaeser¹, Jason D. Tucker¹, Victoria Leroy,
6 Raegan Rawls, Jessalyn Killilee, Molly C. Holbrook, and Qi Long Lu¹

7 ¹McColl-Lockwood Laboratory for Muscular Dystrophy Research, Cannon Research Center,
8 Carolinas Medical Center, Atrium Health, Charlotte, NC 28203, USA.

9
10 Correspondence should be addressed to: Marcela P. Cataldi and Qi Long Lu, McColl-Lockwood
11 Laboratory for Muscular Dystrophy Research, Carolinas Medical Center, Atrium Health,
12 Charlotte, NC 28203, USA

13 E-mail: marcela.cataldi@atriumhealth.org and qi.lu@atriumhealth.org

14 **Short Title:** Ribitol and FKRP therapy for FKRP dystroglycanopathy

15 **Abstract**

16 Mutations in the *FKRP* gene cause dystroglycanopathy with disease severity ranging from
17 mild LGMD2I to severe CMD. Recently, considerable progress has been made in developing
18 experimental therapies, with AAV gene therapy and ribitol treatment demonstrating significant
19 therapeutic effect. However, each treatment has its strengths and weaknesses. AAV gene therapy
20 can achieve normal levels of transgene expression but requires high doses with toxicity concerns
21 and variable distribution. Ribitol relies on residual *FKRP* function and restores limited levels of
22 matriglycan. We hypothesized these two treatments can work synergistically to offer an optimized
23 therapy with efficacy and safety unmatched by each treatment alone. The most effective treatment
24 is the combination of high dose (5e13 vg/kg) AAV-*FKRP* with ribitol, whereas low dose
25 (1e13vg/kg) AAV-*FKRP* combined with ribitol showed 22.6% increase in positive matriglycan
26 fibers and the greater improvement in pathology when compared to low dose AAV-*FKRP* alone.
27 Together, our results support the potential benefits of combining ribitol with AAV gene therapy
28 for treating *FKRP*-related muscular dystrophy. The fact that ribitol is a metabolite in nature and
29 has already been tested in animal models and clinical trials in humans without severe side effects
30 provides a safety profile for it to be trialed in combination with AAV gene therapy.

31 **Introduction**

32 Dystroglycanopathy is a group of muscular dystrophies with defects in glycosylation of
33 alpha dystroglycan (α -DG), which plays a critical role in membrane stability.¹ Fukutin related
34 protein (*FKRP*) gene (OMIM 606596) encodes a ribitol 5-phosphate transferase, which enables
35 the addition of multiple repeats of glucuronic acid (GlcA) and xylose (Xyl) biglycans
36 (matriglycan), which bind many extracellular matrix (ECM) proteins.^{2,3} Mutations in the *FKRP*
37 gene are the most common cause of dystroglycanopathy, which presents a wide spectrum of

38 disease severity.^{4,5} Recently, substantial progress has been made in the development of
39 experimental therapy to FKRP-related dystroglycanopathy. Specifically, our prior study with
40 adeno-associated virus (AAV) gene therapy has demonstrated significant effect to delay and
41 even stop disease progression in mouse models bearing mutations detected in patients.⁶⁻⁹ This
42 line of treatment is currently being pursued in clinical trials both in Europe and North America
43 (ClinicalTrials.gov Identifier: NCT05224505). We also reported that dietary supplementation
44 with the pentose alcohol ribitol, can be readily converted into CDP-ribitol, the substrate of
45 FKRP. Increase in the substrate enhances efficiency of mutant FKRP for the addition of the
46 critical ribitol-5-phosphate to form the functionally glycosylated α -DG.¹⁰ Our *in vivo* studies
47 have shown that, to a limited degree, ribitol can rescue glycosylation defects caused by *FKRP*
48 mutations and preserve muscle function in dystrophic mouse models.¹¹ Further, a phase II
49 clinical trial has reported an increase in the ratio of glycosylated- α -DG over total α -DG,
50 reduction in serum creatine kinase levels, and improvements in functional tests
51 (ClinicalTrials.gov Identifier: NCT04800874 and NCT05775848). However, each of the
52 treatments has its limitations to fulfil the life-long requirement to treat the diseases. AAV gene
53 therapy could restore normal levels of matriglycan in muscles and prevent disease progression in
54 the short-term, but require high dose AAV administration.^{8,9} However, higher doses in AAV
55 gene therapy clinical trials have been associated with side effects of varying degrees of severity,
56 including fatality.¹² Lower doses of AAV are likely to be more safe but produce heterogenous
57 transgene expression among fibers, a great concern for long-term efficacy.

58 The effect of ribitol relies on the residual function of mutant FKRP, limiting its capacity
59 to restore matriglycan expression, especially for a proportion of patients with mutations leading
60 to greatly diminished residual FKRP function.¹³ Fortunately, the endogenous mutant FKRP

61 restores relatively low but homogenously expressed matriglycan in both cardiac and skeletal
62 muscles with ribitol treatment, providing better protection to diseased muscles.

63 We hypothesized that these two therapies can work synergistically to treat FKRP-related
64 dystroglycanopathies with several benefits: ribitol supplementation can stabilize disease
65 progression before gene therapy becomes ready for use; ribitol treatment, after AAV-FKRP gene
66 therapy, can maintain higher and longer therapeutic efficacy. In addition, a lower but
67 homogeneous expression of matriglycan could partially mitigate the damage caused by uneven
68 α -DG glycosylation by AAV gene therapy. Furthermore, the presence of transgene FKRP, even
69 at low levels, could enhance ribitol effect. Thus, this combination might offer an optimized
70 regime consisting of a lower dose and safer AAV treatment, and a long-term lower dose ribitol
71 treatment, with both efficacy and safety unmatched by each treatment alone.

72 In this study, we examined the combined treatment of AAV gene therapy and ribitol in
73 FKRP-P448L mutant mice. Our results confirmed that long-term ribitol treatment alone
74 improves pathology, muscle function and lifespan of dystrophic mice. Combination of AAV-
75 FKRP gene therapy with ribitol showed to be more effective than each treatment alone. Low
76 dose AAV-FKRP (1e13vg/kg) combined with ribitol showed a 22.6% increase in percentage of
77 positive matriglycan fibers and the greater improvement to pathology when compared to low
78 dose AAV-FKRP alone. Together, these results support the therapeutic benefits of a
79 combinatorial approach delivering the functional gene as well as its substrate metabolite to
80 FKRP-related disorders.

81 **Results**

82 We have previously reported that orally administered ribitol is associated with
83 incorporation of ribitol-5-phosphate to α -DG in cardiac and skeletal muscles of the FKRP-P448L

84 mutant mouse (P448L mice). To investigate the potential benefit of ribitol treatment in
85 combination with AAV gene therapy, five-week-old P448L mice were given drinking water
86 supplemented with 5% ribitol and 4 weeks later received a single tail-vein injection of AAV9
87 carrying a codon-optimized, full-length human FKRP coding sequence under control of a
88 **muscle-specific creatin kinase-based promoter (AAV-FKRP)**. Two doses of the AAV-FKRP,
89 1e13vg/kg (FKRP low) and 5e13 vg/kg (FKRP high) were chosen based on our earlier results.
90 The higher dose leads to significant improvement in both pathology and muscle function,
91 whereas the lower dose provides limited protection from disease progression and functional
92 improvement. Oral ribitol treatment continued until the animals were euthanized at 34 or 55
93 weeks of age, reaching 6-month and 1-year post-treatment, respectively.

94 **FKRP gene therapy and Ribitol treatment increase the weight and extend the lifespan of**
95 **dystrophic FKRP-P448L mutant mice**

96 Both ribitol and AAV treatments were associated with an increase in body weight starting
97 from about 1 month after the treatments with the increase becoming more obvious by the
98 termination time points when compared to the untreated control P448L mice (Figure 1A). As
99 expected from our earlier studies, no mouse died at the end of 1 year with all treatments and
100 untreated control. To study the impact of each treatment on the lifespan of the P448L mice we
101 extended the treatment to each cohort with 3 female mice until they reached humane endpoint
102 criteria or a terminal endpoint of 104 weeks according to the IACUC protocol (Figure 1B). The
103 survival of each treated cohort was compared to the lifespan of 10 untreated P448L females,
104 which showed a median survival of 69.5 weeks. The mice treated only with ribitol or AAV at a
105 low dose reached a median survival of 89 and 102 weeks, corresponding to a 28% and 47%
106 increase, respectively. However, all of them reached humane end-point criteria before the

107 predetermined terminal endpoint of 104 weeks. On the other hand, 2 out of 3 females from three
108 treatment cohorts, low dose AAV with ribitol, high dose AAV alone and high dose AAV with
109 ribitol, remained healthy and normally active by 104 weeks of age. These results therefore
110 showed survival benefit of all the treatments regimens, and especially to the cohorts with high
111 dose AAV gene therapy and when ribitol was used in combination with low dose of AAV.
112 Survival of treated male mice was not investigated since untreated P448L male mice have a
113 lifespan of at least 104 weeks.⁹

114 **FKRP gene therapy and ribitol treatment increase matriglycan in cardiac and skeletal** 115 **muscles**

116 Matriglycan expression in cardiac and skeletal muscles was analyzed at both 6 months
117 and 1 year time points with the I1H6C4 monoclonal antibody which specifically recognizes
118 matriglycan, the laminin-binding epitopes of α -DG (Figure 2 and Figure S1). As expected, all
119 mice treated with ribitol, AAV-FKRP, or a combination of both treatments for 6 months showed
120 increased levels of α -DG glycosylation in heart, limb muscle and diaphragm by
121 immunohistochemistry (IHC) when compared to untreated mice (Figure 2A). The signal was of a
122 higher intensity from mice treated with both low and high AAV-FKRP doses when compared to
123 those only drinking ribitol (Figure 2A and 2C). However, the signal from mice treated with
124 ribitol alone was homogeneous in intensity and distribution among most of the fibers in both
125 cardiac and skeletal muscle, whereas matriglycan expression was patchy with a proportion of
126 fibers lacking any positive signals from the muscles with AAV-FKRP treatment, especially at a
127 low dose (Figure 2A). When ribitol treatment was combined with the low dose AAV-FKRP, the
128 contrast between positive and negative fibers appeared less distinct than in AAV low dose alone,
129 likely from the contribution of ribitol and the endogenous mutant FKRP on matriglycan

130 synthesis in fibers that lacked AAV transduction. The I1H6C4 fluorescence intensity per fiber
131 from the IHC assay in TA muscles was analyzed on each treated cohort and untreated P448L
132 mice at 6 months post-treatment (Figure 2B). I1H6C4 mean fluorescence intensity thresholds
133 were stipulated (Figure 2C), and percentage of negative, weak, and bright fibers were quantified
134 per each group (Figure 2D). Of all treated cohorts, mice treated with ribitol alone showed the
135 smaller percentage of brightly positive fibers compared to mice treated with AAV-FKRP at a
136 low or high dose. However, most of the fiber (66.6%) were positive with a weak I1H6C4
137 fluorescent intensity. Mice treated with low dose AAV-FKRP presented 31.5% of negative
138 fibers, the largest amount among all treated cohorts. In mice treated with combination of ribitol
139 and low dose AAV-FKRP, the number of total positive fibers increased to 91% from 68.4% in
140 mice treated with low dose AAV-FKRP alone, with the largest contribution to this increase being
141 from fibers with a weak I1H6C4 intensity.

142 Quantitative differences in levels of matriglycan expression in muscles from different
143 treatment cohorts were confirmed by western blot (WB) with I1H6C4 antibody, and its
144 functionality was further supported by laminin overlay assay (Lam OL) at 6 months and 1-year
145 post-treatment (Figure 2E and 2G, respectively). The levels of matriglycan at 6 months post-
146 treatment showed detectable but limited signal for the ribitol treatment alone (8%, 3% and 11%
147 in heart, TA, and diaphragm, respectively), whereas about 50% of normal levels of matriglycan
148 were detected in both skeletal and cardiac muscles from high dose AAV-FKRP treated mice
149 (Figure 2F). Similar levels of matriglycan were detected between the cohorts of combined
150 treatment, and AAV-FKRP treatment alone. This is likely due to both reduced sensitivity of
151 I1H6C4 antibody in WB compared to IHC and limited increase in matriglycan by ribitol
152 treatment compared to that induced by AAV. By 1 year post treatment, the homogeneity of the

153 increase in levels of matriglycan with ribitol treatment alone became more distinct compared to
154 AAV treated mice, although this level of increase was barely detectable by WB analysis (Figure
155 S1, and Figure 2G, respectively). However, at this time point, the levels of matriglycan in mice
156 with combined treatment of low dose AAV-FKRP and ribitol were 9% and 13% higher in
157 cardiac and TA muscles, respectively, compared to the mice treated with low dose of AAV-
158 FKRP alone (Figure 2H).

159 **Ribitol and AAV-FKRP treatment improve pathology in FKRP-P448L mutant mice**

160 The diaphragm of the P448L mouse exhibits pronounced and progressive fibrosis as the
161 mouse ages. At 6 months after treatment, the diaphragm of the untreated mice had already
162 experienced extensive degeneration and fibrosis which occupied more than 40% of the tissue
163 areas when examined with Masson Trichrome staining (Figure 3A). Improvement in pathology
164 of the mutant mice at this time point was clearly detected with all treatment cohorts (Figure 3A
165 upper panels and 3B left panel). Among the treatments, fibrosis was reduced to 22% in ribitol-
166 treated mice and further lowered to 12% in mice receiving the combined treatment with either a
167 high or low dose of AAV-FKRP. When mice were analyzed after 1-year of treatments (Figure
168 3A lower panels and 3B right panel), the percentage of fibrosis among the treatments was similar
169 to that at 6 months post-treatment, except for mice treated with ribitol alone in which the
170 percentage of fibrosis increased from 22 to 32%.

171 Histological improvements of the dystrophic phenotype of treated P448L mice were
172 demonstrated by hematoxylin and eosin (H&E) staining at 6 months and 1-year post-treatment
173 (Figure 4 and Figure S2, respectively). Consistent with previous reports, untreated mice
174 presented skeletal muscle with large areas of degenerating fibers, high variation in fiber size and

175 a considerable number of centrally nucleated fibers (CNF). Fiber size normal distribution curve
176 analysis showed that all treated cohorts improved the pathology of limb muscles compared to
177 untreated mice, especially after 1 year of treatment, evidenced by the decrease in proportion of
178 small-sized fibers which is the indicator of fiber degeneration and regeneration (Figure 5A, lower
179 panel). Moreover, combined treatment of ribitol with either low or high dose of AAV-FKRP
180 displayed a more homogeneous fiber size distribution overall, compared to untreated mice and
181 mice treated with ribitol or gene therapy alone, with more mid-sized fibers and less small and
182 large diameter fibers as shown by the taller and narrower shape of the curves at both time points.
183 Treated mice also showed decreases in central nucleation in the limb muscle for all cohorts at 6-
184 month time point compared to untreated mice (Figure 5B, upper panel). Ribitol treatment alone
185 reduced CNF from 70% to 52% when compared to untreated mice. Combined treatment of
186 ribitol with lower dose AAV-FKRP showed a decrease on CNF to 33%, a larger improvement
187 compared to ribitol treatment and low dose AAV-FKRP alone (52.3% and 44%, respectively).
188 However, combined treatment with ribitol did not further reduce the percentage of CNF when
189 compared to high dose AAV-FKRP treatment alone. By the 1-year time point, improvement in
190 CNF of the TA muscles was maintained in all cohorts except for ribitol treatment alone which
191 did not show reduction compared to untreated mice (Figure 5B, lower panel).

192 **Ribitol and FKRP gene therapy significantly improve muscle functions**

193 To assess the effect of muscle functions under the treatment regimes, P448L mice were
194 examined at 18, 31 and 52 weeks post-treatment by treadmill exhaustion test, recording running
195 distance and time in comparison with age-matched untreated P448L mice. Significant increase in
196 both running distance and time was observed with the AAV-FKRP treatment alone at both high
197 and low doses compared to untreated mice. Ribitol treatment alone also improved running

198 distance at all three time points but without reaching statistical significance (Figure 6A, upper
199 panel). Interestingly, mice receiving combined high dose AAV-FKRP and ribitol treatment did
200 not show further improvement in performance when compared to mice treated with AAV-FKRP
201 alone at most time points. However, mice treated with low dose of AAV-FKRP in combination
202 with ribitol showed better performance in both running distance and time at 52 weeks compared
203 to the gene therapy alone. This improvement in running distance was more evident when
204 calculated at each time point as fold increase (ratio) compared to the distance run by the
205 untreated mice, indicating better maintenance of muscle function in the mice receiving combined
206 low dose FKRP and ribitol treatment than low dose AAV gene therapy alone (Figure 6B).
207 However, grip force measurement at the same time points showed limited improvement by all
208 the treated cohorts compared to the controls (Figure S3). Nevertheless, this is consistent with our
209 previous results with the same AAV-FKRP gene therapy using the same mouse model.^{8,9}

210 The respiratory muscle function was also examined by non-invasive plethysmography
211 tests at 5 different time points, between 5 and 52 weeks, during the 1-year treatment period
212 (Figure 7). The changes in respiratory function during this period varied with different
213 treatments. Both higher dose of AAV-FKRP alone and with ribitol, as well as low dose AAV-
214 FKRP with ribitol, showed clear improvement in peak inspiratory flow (PIF), expiratory volume
215 (EV), tidal volume (TV), and minute volume (MV), compared to untreated P448L mice. In
216 contrast, lower dose AAV-FKRP alone showed values closer to those of the untreated mice.
217 Interestingly, end inspiratory pause (EIP) and tidal mid-expiratory flow (EF50) increased
218 steadily, especially after 18 weeks of age in the untreated cohort and became the highest at the
219 52-week time point whereas all the treatment cohorts maintained relatively stable levels.
220 Prolonged EIP has been observed in our earlier studies as one of the most significant changes in

221 respiratory function with aging of the P448L mice and shortening of EIP is constantly associated
222 with effective gene therapy.^{9,11}

223 **Effect of Ribitol treatment on AAV-FKRP transduction in skeletal muscle**

224 To assess whether pretreatment with ribitol affects AAV-mediated transgene delivery in
225 muscles, AAV genome copy number was quantified by real-time quantitative PCR (qPCR) in
226 cardiac and skeletal tissues of 55-week-old mice (Figure 8A). We confirmed a dose-dependent
227 increase on AAV-FKRP vector copy number and did not observe any effect of exogenous ribitol
228 on the uptake of AAV-FKRP particles in heart and TA, as shown by the similar number of AAV-
229 FKRP genomes detected in the presence and absence of ribitol at both AAV-FKRP doses.

230 However, when FKRP protein expression was analyzed by JESS simple wester in cardiac tissue
231 of 34 weeks-old mice (55 kDa monomer and 110 kDa dimeric form)¹⁴, we observed an increase
232 on FKRP expression in presence of ribitol, specially at high dose AAV-FKRP (Figure 8B and
233 8C). We have previously reported that ribitol does not affect the endogenous FKRP transcripts
234 levels in cardiac, limb muscle and diaphragm.¹⁰ The reason for the higher FKRP expression in
235 presence of exogenous ribitol in mouse treated with AAV-FKRP is not understood. One
236 hypothesis is that the better improved muscle condition with combined treatment permit better
237 expression of the transgene driven under MCK promoter. This however required further
238 investigation.

239 **Discussion**

240 In this study, we examined effects of combined treatment of AAV gene therapy with
241 ribitol. Consistent with our earlier data, ribitol treatment alone improves pathology and muscle
242 function and AAV-FKRP gene therapy dose-dependently improves muscle pathology and

243 function. These results further support the applications of the individual treatment for LGMD2I
244 and other muscular dystrophies caused by *FKRP* mutations. The most effective treatment is the
245 combination of high dose (5×10^{13} vg/ Kg) AAV gene therapy with ribitol treatment, whereas low
246 dose AAV (1×10^{13} vg/kg) alone showed similar improvements in pathology and function to ribitol
247 treatment alone. This underscores the importance of appropriate AAV dosage for achieving
248 desirable efficacy and the dilemma of balancing high dose treatment and toxicity, especially for
249 treating muscular dystrophy which requires life-long sustained protection. The reasons for
250 increased fibrosis in the diaphragm of ribitol-treated old mice are not understood. One possibility
251 is that the improvement in muscle functions may increase muscle activity causing stress to the
252 muscles with limited matriglycan restoration induced by ribitol treatment at older age. This could
253 lead to further accumulation of damage with regeneration and fibrosis. Increase in CNF in the
254 same aged mice supports this hypothesis.

255 One interesting observation from this study is the differential effect in matriglycan
256 induction and benefit in survival and muscle function between ribitol treatment and lower dose
257 AAV-FKRP gene therapy. Treatment with ribitol alone enhanced matriglycan expression only
258 above the detectable levels. Yet, improvement in muscle function is clearly demonstrated by
259 treadmill exhaustion and respiratory function tests. In contrast, low dose AAV-FKRP treatment
260 induces abundant matriglycan in both skeletal and cardiac muscles in total amount, greatly
261 exceeding the amount induced by ribitol. However, the low dose AAV-FKRP treated mice only
262 showed similar degrees of improvement in muscle and respiratory functions as well as benefit to
263 survival of female mice as that observed with ribitol treatment. The discrepancy between levels
264 of restored matriglycan and muscle function clearly emphasizes the importance of homogenous
265 distribution in therapeutic gene product on efficacy of gene and other therapies as revealed by

266 early studies of dystrophin gene therapy. Rafael et al. described two patterns of dystrophin
267 transgene expression, uniformity and variability.¹⁵ Uniformity refers to transgene expression in
268 nearly 100% of muscle fibers by IHC whereas variable expression observes a mosaic pattern
269 with fibers expressing higher than normal levels adjacent to fibers without positive signal. Mice
270 with uniformly expressed dystrophin are phenotypically indistinguishable from C57, whereas
271 mice with a mosaic pattern of expression remain pathogenic with limited improvement in CNFs
272 and fibrosis evidenced by dystrophic morphology of the diaphragm indistinguishable from
273 parental *mdx* mice. These observations clearly indicate the presence of continuous degeneration
274 and regeneration in the muscles with mosaic pattern of transgene expression. In a follow-up
275 study with the same MCK promotor-driven mini-dystrophin expression, the authors further
276 categorized transduction pattern in muscles as variable, slightly variable or uniform.¹⁶
277 Transgenic animals with uniform expression exhibited the fewest dystrophic symptoms, whereas
278 animals with comparable overall levels of dystrophin in a variable pattern were more severely
279 affected. The authors concluded that uniformity of transgene expression is an important
280 predictor of a therapeutic effect and is more important than the overall level of expression. The
281 limited protection and likely detrimental consequence of heterogeneity in transgene expression
282 by a gene therapy is therefore expected. Over-loading of transprotein is also likely detrimental to
283 the fibers. Further, a mosaic pattern of transgene expression within a single muscle will likely
284 create poorly coordinated contraction, leading to continued fiber damage and degeneration
285 particularly to those fibers or segments of fibers with little and no transgene expression. This
286 process could accelerate with time and diminish the amount of muscle fibers and eventually lead
287 to failure of treatment. In contrast, ribitol treatment produces low levels of matriglycan but with
288 a homogenous distribution, with most fibers expressing similar levels of matriglycan. This may

289 well explain the significant benefit of ribitol treatment despite limited matriglycan induction. It is
290 also important to recall that low levels of endogenous protein expression as therapeutics can
291 provide significant efficacy with other disease related genes.¹⁷ Increased expression of
292 endogenous dystrophin induced by antisense oligonucleotide (ASO) therapy can be difficult to
293 detect especially by WB. More importantly, ASO clinical trials have suggested that barely
294 detectable or even lower than 1% of normal levels in dystrophin upregulation can be associated
295 with clinically meaningful benefits.^{18,19}

296 We hypothesized that ribitol can enhance the function of the transprotein FKRP as well
297 as endogenous mutant FKRP on matriglycan synthesis, thus a combination of the treatments
298 could be more effective to increase the levels of matriglycan. Detection of matriglycan by IHC
299 showed a more homogenously distributed expression in the muscles with combined treatments
300 when compared to the muscles treated only by AAV-FKRP of the same dosage, indicating the
301 contribution of ribitol treatment in the muscles. However, the difference in levels of matriglycan
302 between the AAV-FKRP treated groups with and without ribitol supplementation cannot be
303 demonstrated by WB as clear as by IHC. This is most likely due to limited proportion of
304 matriglycan induced by ribitol in the tissues already with high levels of matriglycan induced by
305 AAV-FKRP alone, and the limited sensitivity of the detection method. It is worthy to note that
306 detection of matriglycan by WB with the currently available IHH6C4 antibody is difficult
307 especially at low level of expression. The nature of the antibody from mouse origin makes it less
308 sensitive to distinguish weak signal from higher background signal in mouse tissues.
309 Nevertheless, the contribution of ribitol to the AAV-FKRP therapy can be appreciated from the
310 greater functional improvements in the combined treatment cohorts compared to AAV-FKRP

311 alone, as indicated by strengthened performance in treadmill exercise tests, better improvements
312 in respiratory functions and muscle pathology.

313 In summary, this study demonstrates the potential benefits of combining ribitol treatment
314 with suboptimal as well as relatively high dosage AAV gene therapy for treating FKRP-related
315 muscular dystrophy. The fact that ribitol is a metabolite in nature and has already been tested
316 both in animal model and clinical trials for more than 1 year without severe side effect provides a
317 safety profile for it to be trialed before and after AAV gene therapy. The results also exemplify
318 the potential of gene therapy in combination with substrate treatment for enhanced efficacy.

319 **Materials and Methods**

320 **Animal care.** All animal studies were approved by the Institutional Animal Care and Use
321 Committee (IACUC) of Carolinas Medical Center and Wake Forest University. All mice were
322 housed in the vivarium of Carolinas Medical Center following animal care guidelines of the
323 institute. Animals were ear tagged prior to group assignment. Food and water were available *ad*
324 *libitum* during all phase of the study. Body weight was measured from 4 weeks of age until
325 experimental or humane endpoint.

326 **Mouse model.** FKRP P448L mutant mice were generated by the McColl-Lockwood Laboratory
327 for Muscular Dystrophy Research.^{20,21} The mouse model contains a homozygous missense
328 mutation (*c.1343C>T*, p.Pro448Leu) in the *FKRP* gene with the floxed neomycin resistant
329 (Neo^r) cassette removed from the insertion site. C57BL/6J (wild-type/C57) mice were purchased
330 from Jackson Laboratory (Bar Harbor, ME) and used as normal controls where appropriate.

331 **AAV Vector and Ribitol administration.** The recombinant AAV-FKRP vector was purchased
332 from ViGene Biosciences (Rockville, MD). Full-length human FKRP cDNA was synthesized for

333 high expression in mouse and subsequently subcloned into a single-stranded AAV9 vector under
334 control of a **muscle-specific promoter**, followed by a polyadenylation signal from the bovine
335 growth hormone gene. The titer of the viral vector stocks was 6.85e13 and 2.32e13 vg/ml. AAV-
336 FKRP was given as a single tail-vein injection to 9-week-old P448L mice, either at a dose of
337 1e13 or 5e13 viral genomes per kilogram of body weight (vg/kg) diluted with 0.9% saline to a
338 final volume of 100 μ l.

339 Ribitol was purchased from Biosynth International, Inc. (A-3000 Adonitol, \geq 98%, Biosynth,
340 Itasca, IL) and dissolved in drinking water to the final concentration of 5%. Water bottles
341 containing ribitol were changed once per week. P448L mice were drinking 5% Ribitol at 5 weeks
342 of age and until natural death or euthanasia.

343 Mice were randomly assigned to either treatment or control groups. No animal was excluded. A
344 total number of 10 mice was used for each group, with equal number of male and female.

345 Untreated age-matched P448L and wild-type C57BL/6 mice were used as controls. Treated and
346 untreated P448L mice were euthanized at 34 (n=3, 2 male and 1 female) or 55 (n=3, 2 male and
347 1 female) weeks of age. For survival studies, mice were euthanized at a terminal endpoint of 104
348 weeks of age, or upon reaching a humane endpoint.

349 **Immunohistochemical, Western Blot, and Jess Simple Western analysis.** Tissues were
350 dissected and snap-frozen in dry-ice-chilled-2-methylbutane. For immunohistochemical
351 detection of glycosylated α -DG, 6 μ m thick cross sections of untreated and treated P448L mice
352 tissues, as well as tissues from C57BL/6 control were included in each slide. Briefly, slides were
353 fixed in ethanol and blocked in blocking buffer (6% bovine serum albumin (BSA), 4% normal
354 goat serum (NGS) in 1x PBS for 30 min at room temperature. Sections were then incubated
355 overnight at 4 $^{\circ}$ C with primary mouse monoclonal antibody I1H6C4 from EMD Millipore

356 (Billerica, MA) against glycosylated α -DG. Sections were then washed 3 times in 1x PBS and
357 incubated with secondary AlexaFluor 488 goat anti-mouse IgM from Invitrogen (Carlsbad, CA)
358 (1:500) at room temperature for 2 h. Sections were washed 3 times in 1x PBS and mounted with
359 fluorescence mounting medium from Abcam (Cambridge, UK) containing 1X DAPI (4',6'-
360 diamidino-2-phenylindole) for nuclear staining. Immunofluorescence was visualized using an
361 Olympus BX51/BX52 fluorescence microscope (Opelco, Dulles, VA) and images were captured
362 using the Olympus DP70 digital camera system (Opelco). For I1H6C4 fluorescence intensity
363 quantification in TA, a total of 3 representative 20x magnification images per animal (a total of
364 300-400 fiber per mice) were analyzed. Using the multi-point selection on ImageJ software, the
365 mean fluorescence intensity from a representative area of the membrane of each fiber was
366 calculated.

367 For western blot analysis, tissues were homogenized in extraction buffer (50 mM Tris-HCl pH
368 8.0, 150 mM NaCl, and 1% Triton X-100), supplemented with 1x protease inhibitor cocktail
369 (Sigma-Aldrich). Protein concentration was quantified by the Bradford assay (Bio-Rad DC
370 protein assay). Fifty μ g of protein was loaded on a 4-15% Bio-Rad Mini-PROTEAN TGX gel
371 (Bio-Rad) and immunoblotted. Amount of total protein loaded for C57BL/6 mice was half of the
372 amount loaded for the P448L mice. Nitrocellulose membranes (Bio-Rad) were blocked with 5%
373 milk in 1x phosphate-buffered saline (PBS) for 2 h at room temperature and then incubated with
374 the following primary antibodies overnight at 4°C: I1H6C4 (1:1000) and α -actin (Sigma)
375 (1:2000). Appropriate horseradish peroxidase (HRP)-conjugated secondary antibodies were
376 incubated for 2 h at room temperature. For laminin overlay assay (Lam OL), nitrocellulose
377 membranes were blocked with laminin overlay buffer (10 mM ethanolamine, 140 mM NaCl, 1
378 mM MgCl₂, and 1 mM CaCl₂, pH 7.4) containing 5% nonfat dry milk for 1 h at 4 °C, followed

379 by incubation with laminin from Engelbreth-Holm-Swarm murine sarcoma basement membrane
380 (Sigma, L2020, 1:500) overnight at 4 °C in laminin overlay buffer. Membranes were then
381 incubated with rabbit anti-laminin antibody (Sigma, L9393, 1:500), followed by goat anti-rabbit
382 HRP-conjugated immunoglobulin G secondary antibody (Santa Cruz Biotechnology, 1:8000).
383 All blots were developed by electrochemiluminescence immunodetection (Perkin-Elmer),
384 exposed to GeneMate auto-radiographic film (VWR International), and subjected to manual film
385 processing. Matriglycan detection with IHH6C4 antibody by western blot analysis was performed
386 on 2-3 mice per treated cohort and untreated control mice.

387 For immunodetection of FKRP in cardiac mouse tissues, we used the ProteinSimple Western
388 JessTM system, an alternative for classical western blotting in which all assay steps from protein
389 separation, immunoprobng, detection, and data analysis are automated. The protein separation
390 was performed using a 12-230 separation kit (Bio-Techne SM-W004-1). Briefly, protein samples
391 were extracted using the previously described method for western blot and diluted to a final
392 concentration of 2 mg/ml in the supplied sample buffer. The primary and secondary antibodies
393 were diluted in milk-free diluent (Bio-Techne 043-524). Rabbit polyclonal FKRP (FKRP-
394 STEM²²) and HSP60 (R&D Systems AF1800) antibodies were diluted to 1:500 and 1:100,
395 respectively, with the anti-rabbit-IgG-NIR secondary (Bio-Techne 043-819), against HSP60
396 primary, diluted to 1:100. The Anti-rabbit-HRP secondary (Bio-Techne 042-206), against FKRP
397 primary, is provided ready to use with no dilution needed. Samples were separated for 25
398 minutes at 375V with a blocking time of 5 minutes, using milk-free antibody diluent. Primary
399 and secondary antibodies were incubated for 30 minutes each. Due to both primary antibodies
400 being rabbit, two separate capillaries were used on the same plate cartridge using the same
401 protein sample.

402 **Histopathological and morphometric analysis.** Frozen tissues were processed for H&E and
403 Masson's Trichrome staining following standard procedures. Muscle cross-sectional fiber
404 equivalent diameter was determined from tibialis anterior stained with H&E using MetaMorph
405 v7.7 Software (Molecular Devices). The percentage of centrally nucleated myofibers were
406 manually quantified from the same tissue sections stained with H&E. Fibrotic area represented
407 by blue staining in the Masson's Trichrome stained sections was quantified from diaphragm
408 using the ImageJ software. For all the morphometric analyses, a total of 300 to 500 fibers from 4
409 representative 20x magnification images per animal were analyzed.

410 **Muscle Function tests.** For treadmill exhaustion test, 18-, 31-, and 52-week-old mice were
411 placed on the belt of a five-lane-motorized treadmill (LE8700 treadmill, Panlab/Harvard
412 Apparatus, Barcelona, Spain) supplied with shock grids mounted at the back of the treadmill,
413 which delivered a 0.2 mA current to provide motivation for exercise. Initially, the mice were
414 subjected to an acclimation period (time, 5 min; speed, 8 cm/s, and 0° incline). Immediately after
415 acclimation period, the test commenced with speed increases of 2 cm/s every minute until
416 exhaustion. The test was stopped and the time to exhaustion was determined when the mouse
417 remained on the shock grid for 5 s without attempting to re-engage the treadmill.⁸

418 **Whole body plethysmography.** Respiratory functional analysis in conscious, freely moving 5-,
419 9-, 18-, 31-, and 52- week-old mice were measured using a whole-body plethysmography
420 technique as described previously.⁸ The plethysmograph apparatus (emka Technologies, Falls
421 Church, VA) was connected to a ventilation pump to maintain a constant air flow, a differential
422 pressure transducer, a usbAMP signal amplifier, and a computer running EMKA iox2 software
423 with the respiratory flow analyzer module, which was used to detect pressure changes due to
424 breathing and recording the transducer signal. An initial amount of 20 ml of air was injected and

425 withdrawn via a 20 ml syringe into the chamber for calibration. Mice were placed inside the free-
426 moving plethysmograph chamber and allowed to acclimate for 5 min to minimize any effects of
427 stress-related changes in ventilation. Resting ventilation was measured for a duration of 15 min
428 after the acclimation period. Body temperatures of all mice were assumed to be 37°C and to
429 remain constant during the ventilation protocol.

430 **Statistical analysis.** All data are expressed as mean \pm SEM unless stated otherwise. Statistical
431 analyses were performed with GraphPad Prism version 7.01 for Windows (GraphPad Software).
432 Individual means were compared using one-way ANOVA with Dunnett's test to correct for
433 multiple comparisons for each treatment versus untreated mice.

434 **Data availability.** The authors declare that all data supporting the findings of this study are
435 available within the article and its Supplemental Information Files.

436 **Author Contributions**

437 Conceptualization, Q.L.L., C.H.V., and M.P.C.; Methodology, Q.L.L., C.H.V., and M.P.C.;
438 Validation, M.P.C.; Formal analysis, M.P.C.; Data acquisition, M.P.C., C.H.V., V.L., R.R., J.K.,
439 and M.H.; Resources, Q.L.L.; Data Curation, M.P.C.; Writing - Review & Editing, M.P.C., A.B.,
440 J.T., and Q.L.L.; Visualization, M.P.C.; Supervision, Q.L.L.; Project Administration, Q.L.L.;
441 Funding Acquisition, Q.L.L.

442 **Conflicts of Interest**

443 Q.L.L. and M.P.C hold patent US-20200061092-A1 (Methods and Compositions for Treating
444 Disorders Associated with Muscle Weakness).

445 **Acknowledgments**

446 This work was supported by the Carolinas Muscular Dystrophy Research Endowment at the
447 Atrium Health Foundation. The authors thanks Natalia Zinchenko (James G. Cannon Research
448 Center Core Histology Laboratory at Carolinas Medical Center) for assistance with histological
449 staining, and the vivarium staff (James G. Cannon Research Center Vivarium at Carolinas
450 Medical Center) for caring for the animals.

451 **Keywords**

452 Dystroglycanopathies, AAV gene therapy, Fukutin-related protein mutations, FKRP-related
453 dystrophy, muscular dystrophy, ribitol, sugar pentose.

454 **References**

- 455 1. Yoshida-Moriguchi, T., and Campbell, K.P. (2015). Matriglycan: a novel polysaccharide that links
456 dystroglycan to the basement membrane. *Glycobiology* 25, 702-713.
- 457 2. Gerin, I., Ury, B., Breloy, I., Bouchet-Seraphin, C., Bolsee, J., Halbout, M., Graff, J., Vertommen,
458 D., Muccioli, G.G., Seta, N., et al. (2016). ISPD produces CDP-ribitol used by FKTN and FKRP to
459 transfer ribitol phosphate onto alpha-dystroglycan. *Nat Commun* 7, 11534.
- 460 3. Kanagawa, M., Kobayashi, K., Tajiri, M., Manya, H., Kuga, A., Yamaguchi, Y., Akasaka-Manya, K.,
461 Furukawa, J., Mizuno, M., Kawakami, H., et al. (2016). Identification of a Post-translational
462 Modification with Ribitol-Phosphate and Its Defect in Muscular Dystrophy. *Cell Rep* 14, 2209-
463 2223.
- 464 4. Brockington, M., Blake, D.J., Prandini, P., Brown, S.C., Torelli, S., Benson, M.A., Ponting, C.P.,
465 Estournet, B., Romero, N.B., Mercuri, E., et al. (2001). Mutations in the fukutin-related protein
466 gene (FKRP) cause a form of congenital muscular dystrophy with secondary laminin alpha2
467 deficiency and abnormal glycosylation of alpha-dystroglycan. *Am J Hum Genet* 69, 1198-1209.
- 468 5. Michele, D.E., Barresi, R., Kanagawa, M., Saito, F., Cohn, R.D., Satz, J.S., Dollar, J., Nishino, I.,
469 Kelley, R.I., Somer, H., et al. (2002). Post-translational disruption of dystroglycan-ligand
470 interactions in congenital muscular dystrophies. *Nature* 418, 417-422.
- 471 6. Xu, L., Lu, P.J., Wang, C.H., Keramaris, E., Qiao, C., Xiao, B., Blake, D.J., Xiao, X., and Lu, Q.L.
472 (2013). Adeno-associated virus 9 mediated FKRP gene therapy restores functional glycosylation
473 of alpha-dystroglycan and improves muscle functions. *Mol Ther* 21, 1832-1840.
- 474 7. Qiao, C., Wang, C.H., Zhao, C., Lu, P., Awano, H., Xiao, B., Li, J., Yuan, Z., Dai, Y., Martin, C.B., et
475 al. (2014). Muscle and heart function restoration in a limb girdle muscular dystrophy 2I
476 (LGMD2I) mouse model by systemic FKRP gene delivery. *Mol Ther* 22, 1890-1899.
- 477 8. Vannoy, C.H., Xiao, W., Lu, P., Xiao, X., and Lu, Q.L. (2017). Efficacy of Gene Therapy Is
478 Dependent on Disease Progression in Dystrophic Mice with Mutations in the FKRP Gene. *Mol
479 Ther Methods Clin Dev* 5, 31-42.

- 480 9. Vannoy, C.H., Leroy, V., and Lu, Q.L. (2018). Dose-Dependent Effects of FKRP Gene-Replacement
 481 Therapy on Functional Rescue and Longevity in Dystrophic Mice. *Mol Ther Methods Clin Dev* **11**,
 482 106-120.
- 483 10. Cataldi, M.P., Lu, P., Blaeser, A., and Lu, Q.L. (2018). Ribitol restores functionally glycosylated
 484 alpha-dystroglycan and improves muscle function in dystrophic FKRP-mutant mice. *Nat*
 485 *Commun* **9**, 3448.
- 486 11. Wu, B., Drains, M., Shah, S.N., Lu, P.J., Leroy, V., Killilee, J., Rawls, R., Tucker, J.D., Blaeser, A.,
 487 and Lu, Q.L. (2022). Ribitol dose-dependently enhances matriglycan expression and improves
 488 muscle function with prolonged life span in limb girdle muscular dystrophy 2I mouse model.
 489 *PLoS One* **17**, e0278482.
- 490 12. Philippidis, A. (2022). Novartis Confirms Deaths of Two Patients Treated with Gene Therapy
 491 Zolgensma. *Hum Gene Ther* **33**, 842-844.
- 492 13. Tucker, J.D., Lu, P.J., Xiao, X., and Lu, Q.L. (2018). Overexpression of Mutant FKRP Restores
 493 Functional Glycosylation and Improves Dystrophic Phenotype in FKRP Mutant Mice. *Mol Ther*
 494 *Nucleic Acids* **11**, 216-227.
- 495 14. Lu, P.J., Zillmer, A., Wu, X., Lochmuller, H., Vachris, J., Blake, D., Chan, Y.M., and Lu, Q.L. (2009).
 496 Mutations alter secretion of fukutin-related protein. *Biochim Biophys Acta* **1802**, 253-258.
- 497 15. Rafael, J.A., Sunada, Y., Cole, N.M., Campbell, K.P., Faulkner, J.A., and Chamberlain, J.S. (1994).
 498 Prevention of dystrophic pathology in mdx mice by a truncated dystrophin isoform. *Hum Mol*
 499 *Genet* **3**, 1725-1733.
- 500 16. Phelps, S.F., Hauser, M.A., Cole, N.M., Rafael, J.A., Hinkle, R.T., Faulkner, J.A., and Chamberlain,
 501 J.S. (1995). Expression of full-length and truncated dystrophin mini-genes in transgenic mdx
 502 mice. *Hum Mol Genet* **4**, 1251-1258.
- 503 17. Marchal, G.A., van Putten, M., Verkerk, A.O., Casini, S., Putker, K., van Amersfoort, S.C.M.,
 504 Aartsma-Rus, A., Lodder, E.M., and Remme, C.A. (2021). Low human dystrophin levels prevent
 505 cardiac electrophysiological and structural remodelling in a Duchenne mouse model. *Sci Rep* **11**,
 506 9779.
- 507 18. Neri, M., Torelli, S., Brown, S., Ugo, I., Sabatelli, P., Merlini, L., Spitali, P., Rimessi, P., Gualandi, F.,
 508 Sewry, C., et al. (2007). Dystrophin levels as low as 30% are sufficient to avoid muscular
 509 dystrophy in the human. *Neuromuscul Disord* **17**, 913-918.
- 510 19. Charleston, J.S., Schnell, F.J., Dworzak, J., Donoghue, C., Lewis, S., Chen, L., Young, G.D., Milici,
 511 A.J., Voss, J., DeAlwis, U., et al. (2018). Eteplirsen treatment for Duchenne muscular dystrophy:
 512 Exon skipping and dystrophin production. *Neurology* **90**, e2146-e2154.
- 513 20. Chan, Y.M., Keramaris-Vrantsis, E., Lidov, H.G., Norton, J.H., Zinchenko, N., Gruber, H.E.,
 514 Thresher, R., Blake, D.J., Ashar, J., Rosenfeld, J., and Lu, Q.L. (2010). Fukutin-related protein is
 515 essential for mouse muscle, brain and eye development and mutation recapitulates the wide
 516 clinical spectrums of dystroglycanopathies. *Hum Mol Genet* **19**, 3995-4006.
- 517 21. Blaeser, A., Keramaris, E., Chan, Y.M., Sparks, S., Cowley, D., Xiao, X., and Lu, Q.L. (2013). Mouse
 518 models of fukutin-related protein mutations show a wide range of disease phenotypes. *Hum*
 519 *Genet* **132**, 923-934.
- 520 22. Esapa, C.T., McIlhinney, R.A., and Blake, D.J. (2005). Fukutin-related protein mutations that
 521 cause congenital muscular dystrophy result in ER-retention of the mutant protein in cultured
 522 cells. *Hum Mol Genet* **14**, 295-305.

523 Figure legends

524 **Figure 1. Effect of Ribitol and AAV-FKRP treatment on body weight and lifespan of**
525 **P448L mutant mice.** Mice were treated with 5% ribitol in drinking water (RIBITOL), a single
526 dose of $1e13$ or $5e13$ vg/kg AAV-FKRP (FKRP low and FKRP high, respectively), or combined
527 treatment of 5% ribitol and either $1e13$ or $5e13$ vg/kg AAV-FKRP (RIBITOL + FKRP low and
528 RIBITOL + FKRP high, respectively). Treated cohorts were compared to age-matched control
529 mice (UNTREATED). **(A)** Body weight (gr) comparison among mice treated as described above
530 (Female: $n = 5$ up to 6 months of age; $n = 4$ from 6 months to 12 months of age; $n = 3$ starting at
531 12 months of age; Male: $n = 5$ up to 6 months of age; $n = 3$ from 6 months to 12 months of age).
532 Mice died by natural cause or were euthanized by either reaching humane endpoint criteria or a
533 predetermined terminal endpoint of 34, 55 or 104 weeks). **(B)** Kaplan-Meier survival curve of
534 female P448L mutant mice treated as described above ($n = 10$ for untreated mice; $n = 3$ for all
535 treated cohorts). Mice died by natural cause or were euthanized by either reaching humane
536 endpoint criteria or the predetermined terminal endpoint of 104 weeks.

537 **Figure 2: Induction of matriglycan in cardiac and skeletal muscle of P448L mice treated**
538 **with Ribitol and AAV-FKRP gene therapy for 6 months and 1 year.** Five % Ribitol was
539 supplemented in drinking water at 5 weeks of age (RIBITOL). AAV-FKRP was administered
540 systemically as a single dose at $1e13$ (FKRP low) or $5e13$ vg/kg (FKRP high) at 9 weeks of age.
541 Mice under combined therapy were drinking 5% ribitol and received AAV-FKRP either at $1e13$
542 or $5e13$ vg/kg (RIBITOL + FKRP low and RIBITOL + FKRP high, respectively). **(A)**
543 Immunohistochemical staining with I1H6C4 antibody of cardiac (HEART), tibialis anterior (TA)
544 and diaphragm (DIAPH) of treated and age-matched untreated P448L mice at 34 weeks of age.
545 Arrows indicate negative fibers in AAV-FKRP alone treatment compared to weak stained fiber
546 in AAV-FKRP and ribitol combined therapy. DAPI was used for nuclear staining. **(B, C, D)**

547 Quantification of matriglycan by I1H6C4 fluorescence intensity in TA of treated and age-
548 matched untreated P448L mice at 34 weeks of age ($n = 3$ per each cohort). (B) Histogram of
549 fiber frequency distribution as percentage. (C) Nonlinear Gaussian Regression fitting histogram
550 showed in B. Dotted lines represent thresholds between negative and positive (weak and strong)
551 fibers. (D) Stacked-bar graph representing percentage of fibers with I1H6C4 fluorescence intensity
552 calculated in B (Negative fiber: I1H6C4 mean intensity <10 ; positive weak fiber: I1H6C4 mean
553 intensity between 10 and 30; positive bright fiber: I1H6C4 mean intensity >30). (E, F) Western
554 blot analysis of protein lysates from untreated and treated mice at 34 weeks of age. Matriglycan
555 was detected by blotting with I1H6C4 and by laminin overlay assay (Lam OL). Detection of α -
556 actin was used as loading control. (F) Quantification of I1H6C4 band intensity showed in (E),
557 normalized to α -actin expression for each tissue showed as percentage of levels in C57 mice. (G,
558 H) Western blot analysis of protein lysates from untreated and treated mice at 55 weeks of age.
559 Matriglycan was detected by blotting with I1H6C4 and by laminin overlay assay (Lam OL).
560 Detection of α -actin was used as loading control. (H) Quantification of I1H6C4 band intensity
561 showed in (G), normalized to α -actin expression for each tissue showed as percentage of levels
562 in C57 mice. The western blot figures show representative data analyzed for 2-3 mice per cohort.

563 **Figure 3: Effect of Ribitol and AAV-FKRP Gene Therapy on the progression of fibrosis in**
564 **diaphragm of P448L mice.** Mice were treated with 5% ribitol in drinking water (RIBITOL), a
565 single dose of $1e13$ or $5e13$ vg/kg AAV-FKRP (FKRP low and FKRP high, respectively), or
566 combined treatment of 5% ribitol and either $1e13$ or $5e13$ vg/kg AAV-FKRP (RIBITOL + FKRP
567 low and RIBITOL + FKRP high, respectively). (A) Masson's Trichrome staining in diaphragms
568 of treated and age-matched untreated P448L mice, as well as C57BL/6 control mice, at 34-week
569 (upper panels) and 55-week (lower panel) of age. Scale bar, 50 μ m. (B) Percentage of fibrotic

570 areas quantified from Masson's Trichrome staining in diaphragm of untreated and treated mice at
571 34 weeks (left panel) and 55 weeks (right panel) of age. Four representative 20x magnification
572 images per animal were analyzed. ($n = 3$ per each cohort). Error bars represent mean \pm SEM.
573 (**) $p \leq 0.01$, (****) $p \leq 0.0001$, one-way ANOVA with Dunnett's test to correct for multiple
574 comparisons for each treatment versus untreated mice.

575 **Figure 4: Histopathology of muscle tissues from P448L mice treated with Ribitol and AAV-**
576 **FKRP for 6 months.** H&E staining of heart, tibialis anterior (TA) and diaphragm (DIAPH)
577 tissues from 34 weeks old control P448L mice (Untreated), or mice treated with 5% ribitol in
578 drinking water (Ribitol), mice injected with $1e13$ or $5e13$ vg/kg AAV-FKRP (FKRP low and
579 FKRP high, respectively), or mice receiving combined treatment of 5% ribitol plus either $1e13$ or
580 $5e13$ vg/kg AAV-FKRP (R + FKRP low and R + FKRP high, respectively). Scale bar, $50\mu\text{m}$.

581 **Figure 5: Effect of Ribitol and AAV-FKRP gene therapy on fiber size distribution and**
582 **centrally nucleated fibers of P448L mice treated for 6 months and 1 year.** (A) Gaussian fiber
583 size distribution as percentage of relative frequency in tibialis anterior muscles of either treated
584 or untreated P448L mice, and C57 control, at 6-month and 1-year post-treatment (upper panel
585 and lower panel, respectively). Mice were treated with 5% ribitol in drinking water (RIBITOL),
586 a single dose of $1e13$ or $5e13$ vg/kg AAV-FKRP (FKRP low and FKRP high, respectively), or
587 combined treatment of 5% ribitol and either $1e13$ or $5e13$ vg/kg AAV-FKRP (RIBITOL + FKRP
588 low and RIBITOL + FKRP high, respectively) ($n = 3$ per each cohort). (B) Percentage of fibers
589 with central nucleation in tibialis anterior muscles of P448L mice untreated or treated as
590 described in (A) by 6-months and 1-year post treatment (upper panel and lower panel,
591 respectively) ($n = 3$ per each cohort). Error bars represent mean \pm SEM. (*) $p \leq 0.05$, (**) $p \leq 0.01$,

592 one-way ANOVA with Dunnett's test to correct for multiple comparisons for each treatment
593 versus untreated mice.

594 **Figure 6: Effect of Ribitol and AAV-FKRP gene therapy on skeletal muscle function on**

595 **P448L mice. (A)** Treadmill exhaustion test assessing running distance (m) and time (min) in

596 treated and age-matched untreated P448L mice. Ribitol-treated mice drank 5% ribitol

597 (RIBITOL). AAV-FKRP-treated mice received a single dose of $1e13$ or $5e13$ vg/kg (FKRP low

598 and FKRP high, respectively). Mice receiving the combined treatment were injected with a

599 single dose of $1e13$ or $5e13$ vg/kg AAV-FKRP and drank 5% (RIBITOL + FKRP low and

600 RIBITOL + FKRP high, respectively). Test was performed at 18, 31, and 52 weeks of age (18w,

601 31w, and 52 weeks, respectively). ($n = 10$ per each cohort at 18w and 31w time point, and $n = 7$

602 per each cohort at 52w time point). Error bars represent mean \pm SEM. (*) $p \leq 0.05$, (**) $p \leq 0.01$,

603 (***) $p \leq 0.001$, (****) $p \leq 0.0001$, one-way ANOVA with Dunnett's test to correct for multiple

604 comparisons for each treatment versus age-matched untreated mice. **(B)** Distance running

605 progression by each treated cohort normalized to the distance run by untreated mice at each time

606 point.

607 **Figure 7. Evaluation of respiratory function in P448L mice treated with Ribitol and AAV-**

608 **FKRP gene therapy.** Plethysmography test was conducted in treated and age-matched untreated

609 P448L mice at different times of age (x axis represents the mice age in weeks). Data obtained at

610 5 weeks of age (before treatment started) was used as base line and subtracted from each time

611 point per each mouse. ($n = 10$ per each cohort at 5-, 9-, 18- and 31-week time points, and $n = 7$

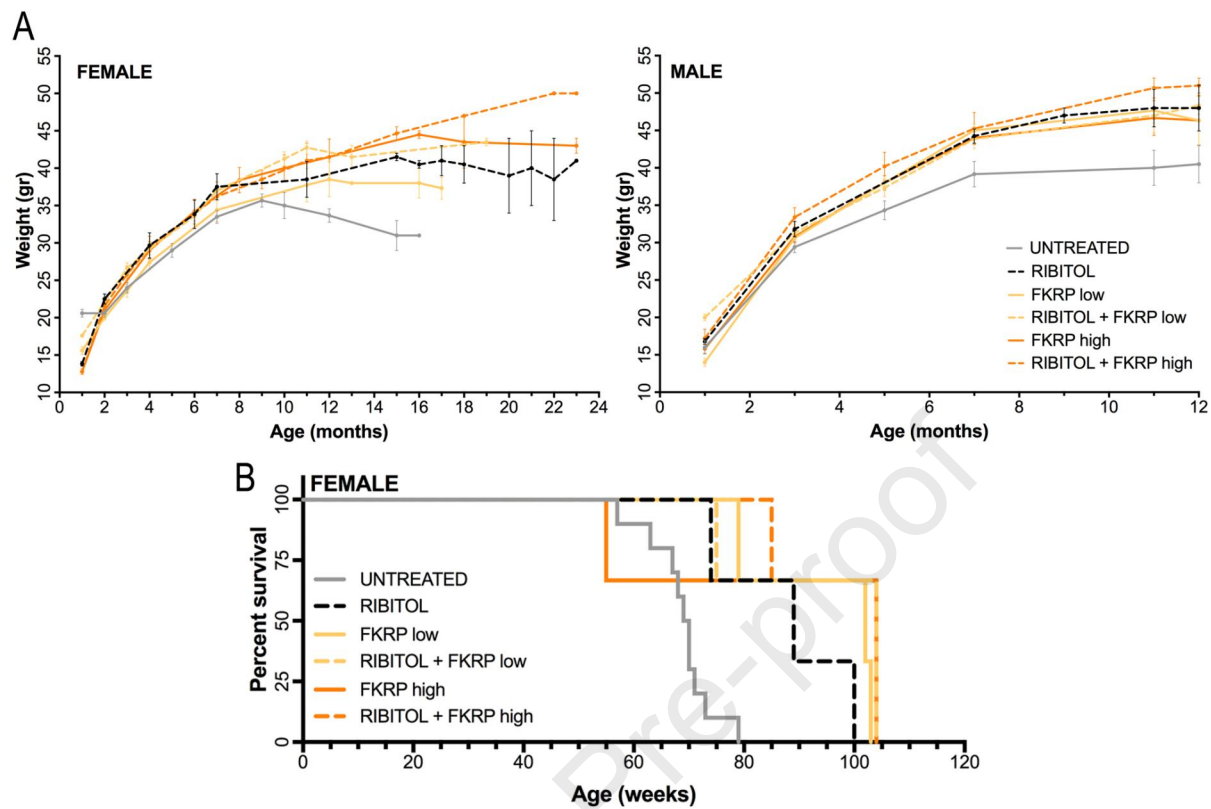
612 per each cohort at 52-week time point). Ribitol-treated mice drank 5% ribitol (RIBITOL). AAV-

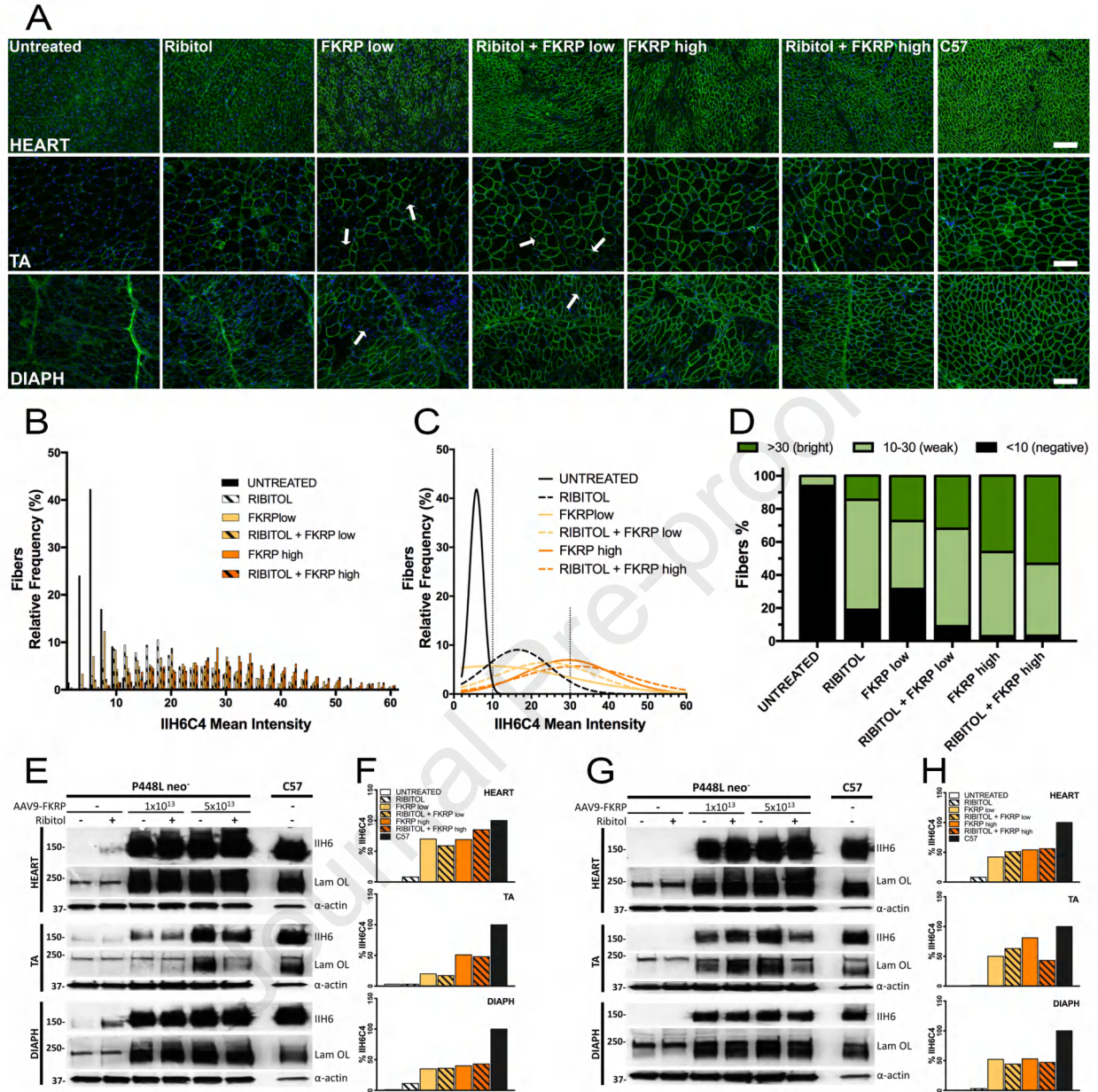
613 FKRP-treated mice received a single dose of $1e13$ or $5e13$ vg/kg (FKRP low and FKRP high,

614 respectively). Mice receiving the combined treatment were injected with a single dose of $1e13$ or

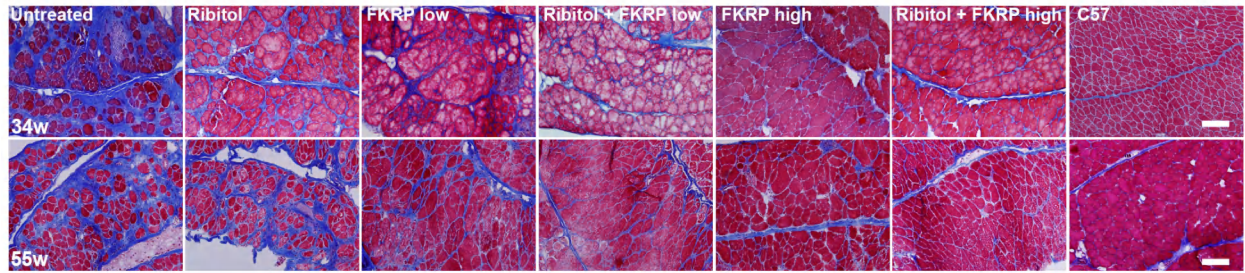
615 5e13 vg/kg AAV-FKRP and drank 5% ribitol (RIBITOL + FKRP low and RIBITOL + FKRP
616 high, respectively). Error bars represent mean \pm SEM. PIF, peak inspiratory flow (ml/s); EV,
617 expired volume (ml); TV, tidal volume (ml); EIP; endo-inspiratory pause (msec); MV, minute
618 volume (ml); EF50, mid-expiratory flow (ml/s).

619 **Figure 8. Effect of Ribitol on AAV-FKRP transduction efficiency.** (A) Vector copy number
620 per μ g of input DNA in heart and skeletal (TA = tibialis anterior) tissues from P448L mice
621 treated with AAV-FKRP alone (FKRP low: 1e13 vg/kg; FKRP high: 5e13 vg/kg) and combined
622 with 5% ribitol treatment (Ribitol + FKRP low and Ribitol + FKRP high) at 55-week of age (n =
623 3). Error bars represent mean \pm SEM. (B) FKRP protein levels from cardiac tissue of 34-week-
624 old treated and untreated P448L mice analyzed by ProteinSimple JessTM Capillary Western Blot
625 analyzer. Detection of HSP60 was used as loading control. (C) Quantification of FKRP band
626 intensity showed on (B). Values were normalized to HSP60 expression for each tissue.

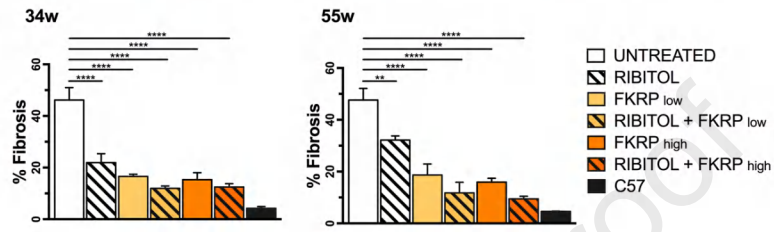


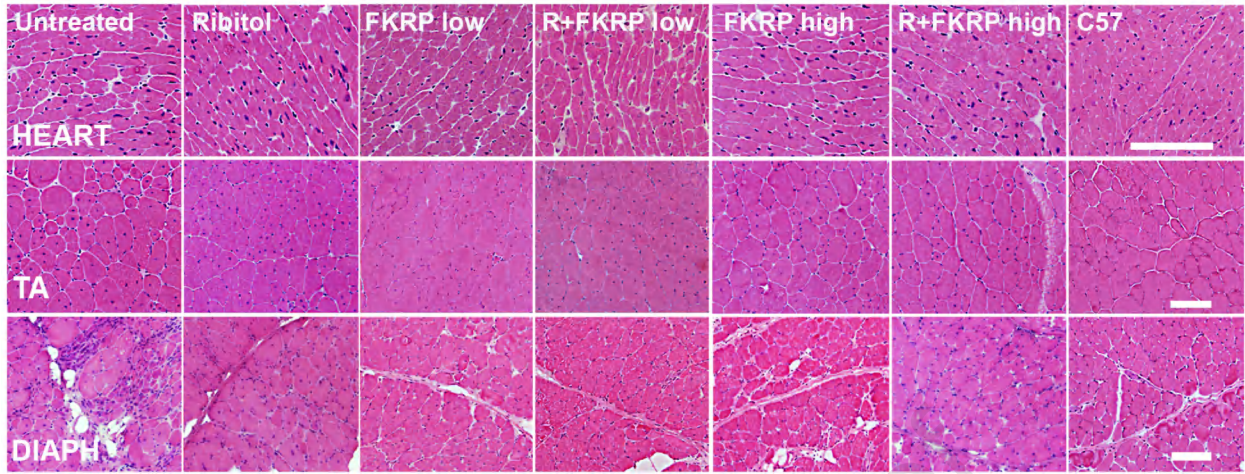


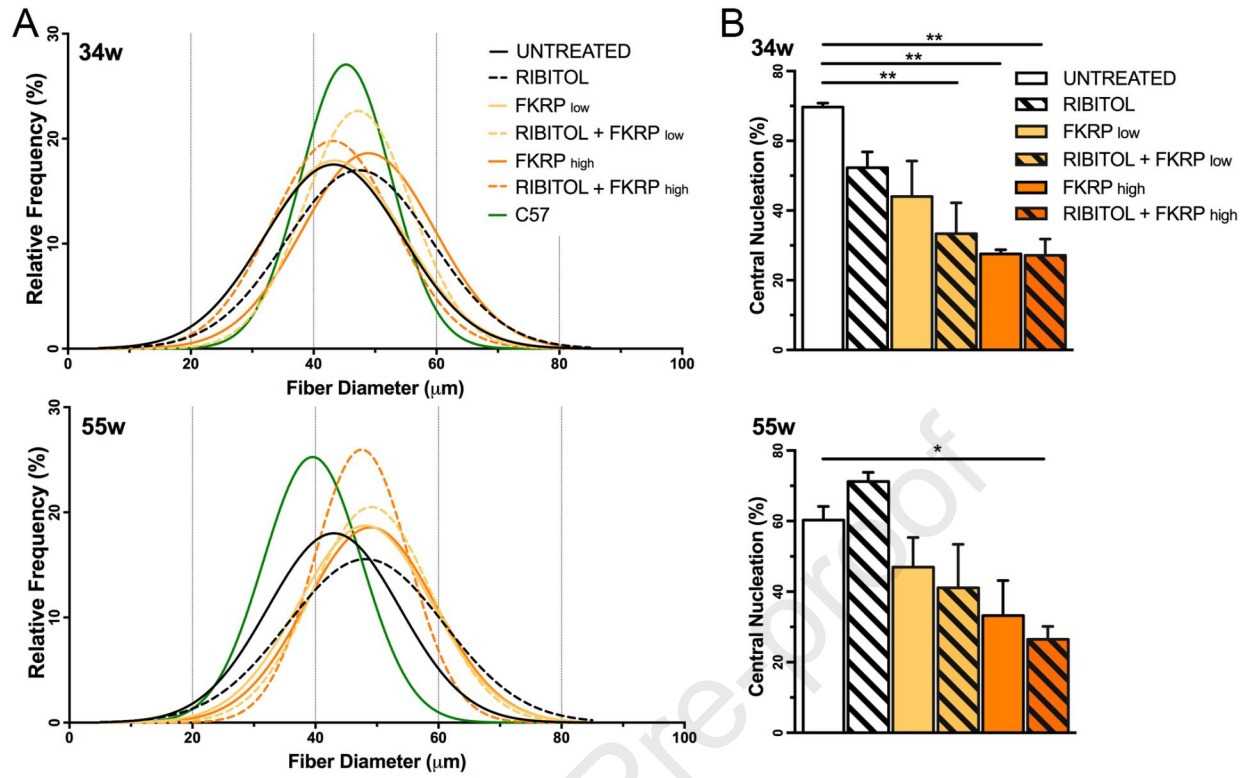
A

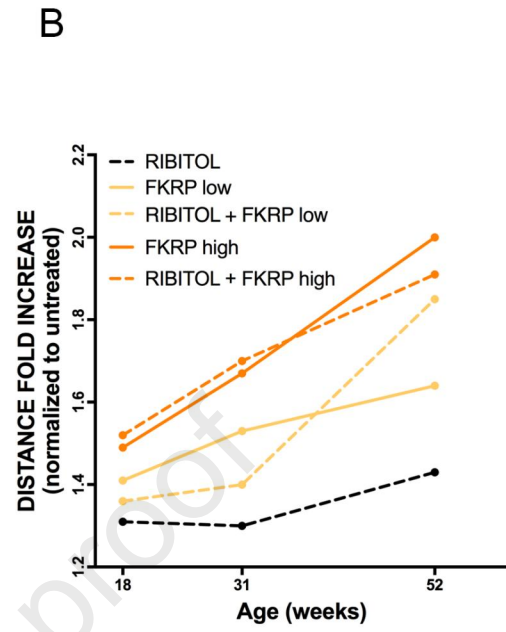
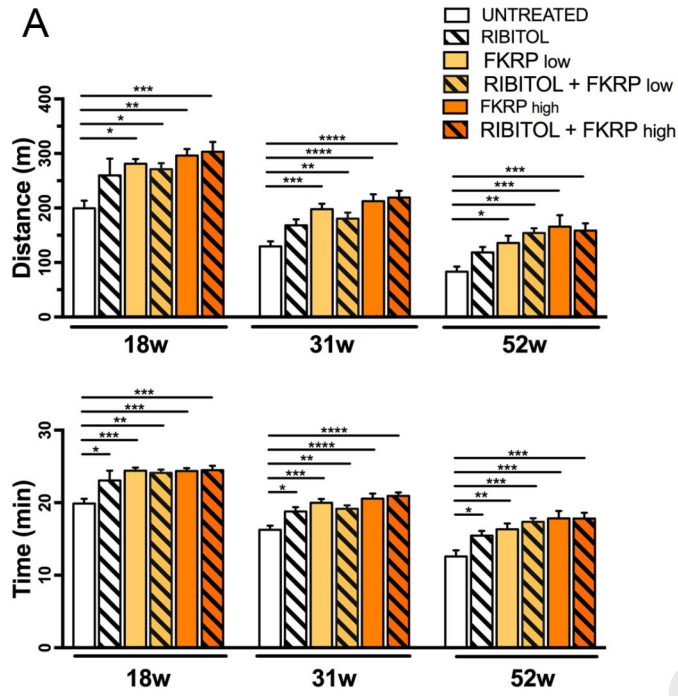


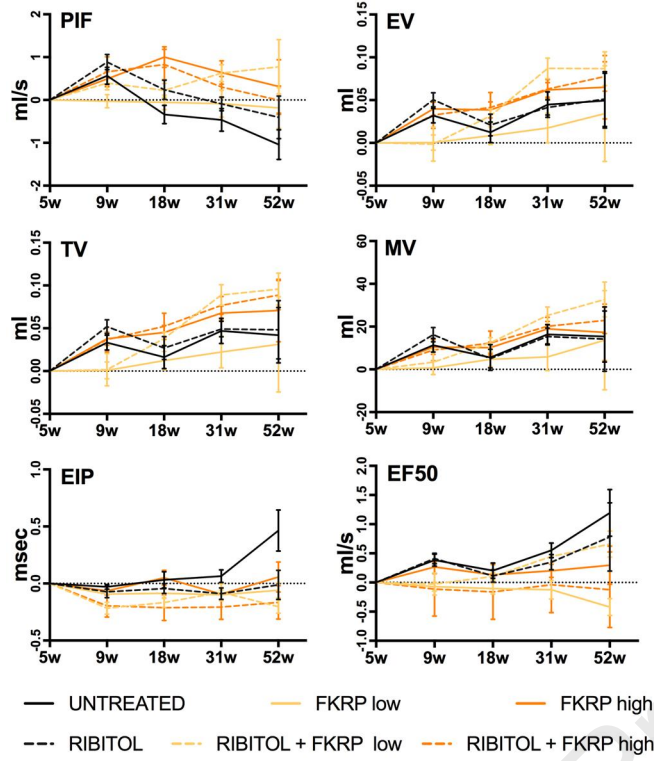
B



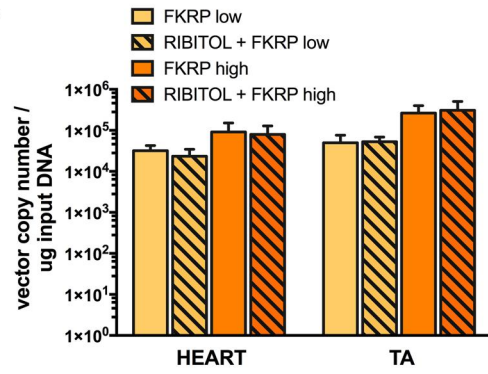




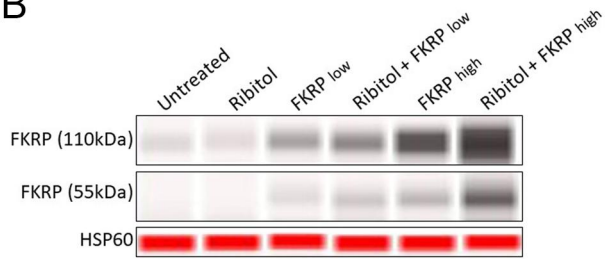




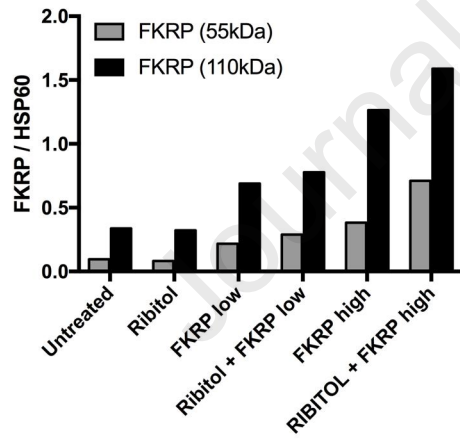
A



B



C



Cataldi and colleagues report that combining AAV gene therapy and Ribitol treatment for FKRP-related dystroglycanopathies result in an optimized therapy compared to each treatment alone. Ribitol increases FKRP's substrate pool while AAV-mediated FKRP expression compensates for mutant FKRP, improving pathology, muscle function and survival in a FKRP-dystrophic mouse model.

Journal Pre-proof